Sensitivity analysis of temperature changes for determining thermal properties of partially frozen soil with a dual probe heat pulse sensor

Yuki Kojima, Joshua L. Heitman, Kosuke Noborio, Tusheng Ren, Robert Horton

PII: S0165-232X(17)30434-2
DOI: doi:10.1016/j.coldregions.2018.03.022
Reference: COLTEC 2562

To appear in: *Cold Regions Science and Technology*

Received date: 19 September 2017
Revised date: 16 February 2018
Accepted date: 22 March 2018

Please cite this article as: Yuki Kojima, Joshua L. Heitman, Kosuke Noborio, Tusheng Ren, Robert Horton , Sensitivity analysis of temperature changes for determining thermal properties of partially frozen soil with a dual probe heat pulse sensor. The address for the corresponding author was captured as affiliation for all authors. Please check if appropriate. Coltec(2018), doi:10.1016/j.coldregions.2018.03.022

Sensitivity Analysis of Temperature Changes for Determining Thermal Properties of Partially Frozen Soil with a Dual Probe Heat Pulse Sensor

Yuki Kojima*[a], Joshua L. Heitman[b], Kosuke Noborio[c], Tusheng Ren[d], and Robert Horton[e]

a) The Department of Civil Engineering, Gifu University, 1-1 Yanagido, Gifu City, Gifu 501-1193, Japan (email: kojima@gifu-u.ac.jp)

b) The Department of Soil Science, North Carolina State University, Raleigh, NC 27695, USA (e-mail: jlheitma@ncsu.edu)

c) The School of Agriculture, Meiji University, 1-1-1 Higashimita, Tama-ku, Kawasaki City, Kanagawa 214-8571, Japan (email: noboriok@meiji.ac.jp)

d) The Department of Soil and Water Sciences, China Agricultural University, Beijing 100193, China (e-mail: tsren@cau.edu.cn)

e) The Department of Agronomy, Iowa State University, Ames, IA 50011, USA (e-mail: rhorton@iastate.edu)

* Corresponding author

Abstract

Determining thermal conductivity (λ) and volumetric heat capacity (C) of partially frozen soils with a dual probe heat pulse (DPHP) sensor is challenging because an applied heat pulse melts ice surrounding the heater probe. Examining DPHP temperature changes with a commonly-used analytical solution that only accounts for heat conduction leads to inaccurate λ and C estimates for partially frozen soils at temperatures between −5°C and 0°C. In order to determine λ and C accurately and simultaneously, it is necessary to understand how various properties of partially frozen soil influence the temperature changes produced by DPHP sensors. The objective of this study is to determine the sensitivity of DPHP temperature changes to soil conditions and soil thermal properties. A numerical solution for radial heat conduction with soil freezing and thawing is developed. A series of simulations are performed, in which various errors are imposed onto a selected model parameter while other model parameters are held constant, and sensitivity coefficient values (φ) of the time of maximum probe temperature (t_m) and of the maximum probe temperature rise (T_m) for each parameter are calculated. Temperature changes at the measurement probe are quite sensitive to initial soil temperature (φ values for t_m and for T_m are −0.99 and 0.99, respectively), λ (φ value for t_m is −0.93), and parameters determining the shape of the soil freezing characteristic (FC) curve, i.e., saturated water content θ_s (φ values for t_m and for T_m are 0.59 and −0.73, respectively) and n (φ values for t_m and for T_m are −2.7 and 2.4, respectively). Temperature changes are not very sensitive to C (φ values for t_m and for T_m are 0.034

and −0.15, respectively). Although previous investigations tried to determine *C* by inverse analysis, this sensitivity analysis shows that the influence of *C* on temperature response to a heat pulse is masked by that of the FC. Thus, λ and FC parameters are the best candidate parameters to be determined by inverse analysis of DPHP data. This new result will guide further testing of DPHP sensors in partially frozen soils.

Keywords: partially frozen soil; thermal conductivity; volumetric heat capacity; dual probe heat pulse; freezing characteristic

Abbreviations

DPHP, dual probe heat pulse; FC, freezing characteristic; PILSS, pulsed infinite line source solution

Introduction

Soil freezing and thawing impacts soil hydrology. Since soil freezing and thawing involves coupled heat and water transfer, understanding heat transfer in partially frozen soils is important for modeling, predicting, and interpreting winter hydraulic processes in partially frozen soils. Knowing soil thermal properties is fundamental for understanding soil heat transfer, and the dual probe heat pulse (DPHP; Campbell et al., 1991; Bristow et al., 1994) methods have been widely used for simultaneous measurement of soil thermal conductivity (λ) and volumetric heat capacity (C) (e.g., Bilskie et al., 1998; Ochsner et al., 2001; Ren et al., 2003; Heitman et al., 2008a, 2008b; Xiao et al., 2011). However, measuring thermal properties of partially frozen soil with a DPHP is difficult, in particular, when soil temperature is slightly less than 0ºC.

The DPHP approach determines λ and C by analyzing heat pulse induced temperature changes at a temperature measurement probe located at a known distance from the heater probe. An analytical solution, i.e., the pulsed infinite line source solution (PILSS; Kluitenberg et al., 1993), is used to analyze the temperature change with time data. The PILSS accounts for conductive heat transfer, but ignores latent heat associated with the phase change of water. When DPHP sensors are used in partially frozen soil, ice melting violates the assumption of the PILSS that there is no phase change of water, and they estimate inaccurate thermal properties. The error associated with the ice melting and use of PILSS is large when soil temperature is slightly less than 0ºC because of the dynamic ice melting caused by

heating.

Ochsner and Baker (2008) reported that partially frozen soil λ and *C* are both overestimated with DPHP sensors. The overestimated λ and *C* were referred to as apparent thermal conductivity and apparent volumetric heat capacity. Overestimation of λ was mostly observed at temperatures between −2°C and 0°C (Kojima et al., 2016). Putokonen (2003) reported that *C* was overestimated in the temperature range between −10°C and 0°C. Some studies determined soil ice content based on measurement of *C* with DPHP sensors (Liu and Si, 2011; Zhang et al., 2011; Tian et al., 2015). Zhang et al. (2011) found that the ice content of sand based on *C* measured with DPHP sensors was inaccurate at temperatures between −2°C and 0°C. Tian et al. (2015) used several soils and concluded that the errors associated with ice melting were not significant at temperatures below −5°C when heat application was carefully controlled. He et al. (2015) quantified the amount of ice melting due to heat pulses in partially frozen soil and concluded that the ice melting primarily occurred at temperatures between −5°C and 0°C.

Accurate determination of λ and *C* simultaneously at temperatures between −5°C and 0°C remains a challenge. Understanding how various properties of partially frozen soil influence the temperature changes for DPHP measurements is necessary to achieve accurate and simultaneous determination of λ and *C*. The objective of this study is to examine the sensitivity of DPHP temperature changes to various soil properties. The sensitivity analysis is performed with a developed numerical

solution for radial heat conduction during water freezing and thawing.

Materials and Methods

Numerical model for radial heat conduction with freezing and thawing

There are several numerical codes for one-dimensional soil water and heat transfer involving freezing and thawing, e.g., simultaneous heat and water (SHAW) model (Flerchinger and Saxton, 1989), COUP model (Jansson and Karlberg, 2001), and HYDRUS-1D freezing/thawing module (Hansson et al., 2004). However, heat pulse probe measurements produce two-dimensional radial heat transfer in soil which one-dimensional models cannot simulate accurately. Therefore, we developed a numerical model that considers radial heat transfer involving freezing and thawing of soil water. A numerical solution for radial heat conduction with water freezing and thawing is developed using MATLAB ver. R2015a (MathWorks, Inc., Natick, USA). Radial heat conduction with water phase change is described as (Patanker, 1980)

$$C\frac{\partial T}{\partial t}-\rho_{\mathrm{I}}L_{\mathrm{f}}\frac{\partial \theta_{\mathrm{I}}}{\partial t}=\frac{1}{r}\frac{\partial}{\partial r}\left(r\lambda\frac{\partial T}{\partial r}\right) \qquad [1]$$

where C is soil volumetric heat capacity (J m^{-3} °C^{-1}), T is soil temperature (°C), t is time (s), ρ_{I} is the density of ice (kg m^{-3}), L_{f} the is latent heat of fusion (J kg^{-1}), θ_{I} is volumetric ice content (m^3 m^{-3}), r is radial distance from the center (m), and λ is soil thermal conductivity (W m^{-1} °C^{-1}). Equation [1] is solved with a finite difference method (implicit Crank-Nicolson scheme). Figure 1 shows a diagram of

the discretized areas and nodes representing each area. The radial heat conduction is two dimensional, however, it can be treated as one dimensional radial heat conduction by assuming homogenous thermal properties and temperature for each targeted area in Fig. 1.

A discretized form of Eq. [1] for the numerical solution is described as (Patanker, 1980)

$$C\Delta A\frac{\Delta T_i}{\Delta t}-\rho_{\mathrm{I}}L_{\mathrm{f}}\Delta A\frac{\Delta\theta_{\mathrm{I},i}}{\Delta t}=2\pi r_i\lambda_i\frac{T_{i+1}-T_i}{\delta r_i}+2\pi r_{i-1}\lambda_{i-1}\frac{T_{i-1}-T_i}{\delta r_{i-1}} \qquad [2]$$

where ΔA is the control area that equals to $(r_i+r_{i-1})\pi\Delta r$ (m^2), and subscript i represents the discretized area number. The first and second terms on the left hand side of Eq. [2] express sensible heat storage and latent heat sink/source, respectively. When the soil is unfrozen, the second term is equal to zero. On the right hand side of the equation, the first and second terms show conductive heat fluxes at the boundaries. To determine ice content θ_I, the soil freezing characteristic (FC) that expresses the relationship between liquid water content θ_L (m^3 m^{-3}) and temperature T (°C) of partially frozen soil, is required. By subtracting θ_L, determined by T and the FC, from θ_T, θ_I is determined (i.e., $\theta_I = \theta_T - \theta_L$). Thus, $\Delta\theta_I/\Delta t$ is determined by T at two consecutive time steps.

The similarity of the FC and the water characteristic curve has been reported (e.g., Spaans and Baker, 1996), and often the FC is estimated from the water characteristic curve with matric potentials, ψ, converted to temperature by using the Clausius-Clapeyron equation (e.g., Kurylyk and Watanabe, 2013; Kojima et al., 2016);

$$\psi = \frac{L_f}{g}\left(\frac{T}{273.15\,°C}\right) \qquad [4]$$

where g is the gravitational acceleration (9.8 m s^{-2}). Flerchinger et al. (1989) use the Brooks and Corey (1964) model to describe the FC for the SHAW model, and Hansson et al. (2004) incorporate the van Genuchten (1980) model for soil freezing in HYDRUS-1D. In this study, the van Genuchten (1980) model for the water characteristic curve is revised as follows to describe the freezing characteristic curve:

$$\theta_L = \theta_r + (\theta_s - \theta_r)\left[\frac{1}{1+|\alpha T|^n}\right]^{1-1/n} \qquad [3]$$

where θ_s is the saturated water content (m^3 m^{-3}) and θ_r is the residual water content (m^3 m^{-3}), and α and n are empirical parameters that are determined by fitting Eq. [3] to the water characteristic curve of a Nicollet sandy clay loam (a fine-loamy, mixed, superactive, mesic Aquic Hapludoll) soil shown in Fig.2. Equation [3] treats θ_L as a function of only soil temperature. The FC curve might be slightly affected by soil ice pressure and osmotic potential of liquid water (Spaans and Baker, 1996), but these effects were assumed to be negligible.

Soil thermal properties, C and λ, are functions of θ_I, θ_L and bulk density ρ_b (kg m^{-3}). Volumetric heat capacity is calculated by the de Vries (1963) model,

$$C = \rho_b c_s + \theta_L C_L + \theta_I C_I \qquad [5]$$

where c_s is the specific heat of soil solids (J kg^{-1} $°C^{-1}$), and C_L and C_I are volumetric heat capacity of

liquid water and ice (J m^{-3} °C^{-1}), respectively. The Nicollet sandy clay loam has a bulk density of 1.2×10^3 kg m^{-3}. The c_s is assumed to be 8.79×10^2 J kg^{-1} °C^{-1} based on soil texture and organic matter content of the sandy clay loam (Kojima et al., 2014). The values for C_L and C_I are 4.21×10^6 J m^{-3} °C^{-1} at 0°C and 1.87×10^6 J m^{-3} °C^{-1} at −10°C, respectively (Farouki, 1986). The Hansson et al. (2004) model is used to calculate λ;

$$\lambda = c_1 + c_2\left(\theta_L + F\theta_I\right) - (c_1 - c_4)\exp\left\{-\left[c_3\left(\theta_L + F\theta_I\right)\right]^{c_5}\right\} \quad [6]$$

where c_1, c_2, c_3, c_4, and c_5 are empirical parameters, and F is a function described as

$$F = 1 + F_1\theta_I^{F_2} \quad [7]$$

where F_1 and F_2 are also empirical parameters. The empirical parameters are determined by fitting Eqs. [6, 7] to observed data for Nicollet sandy clay loam. The observed data and fitting results are shown in Fig. 3. Soil information and empirical parameters for the Nicollet sandy clay loam are listed in Table 1.

The center node is assumed to be the location of the heater probe, which has a diameter of 1.27 mm and is assumed to be a perfect heat conductor, i.e., probe thermal conductivity is infinite. Volumetric heat capacity of the heater probe, 2.84 MJ m^{-3} °C^{-1}, is taken from Knight et al. (2012). Node spacing is 0.77 mm between the first (center) node and the second node, and it is 0.28 mm for the others. The node spacing was established to have 20 nodes between the center node and a node at 6 mm away from the center, which is a typical probe spacing. The first node spacing is larger than the others because the model takes the existence of the heater needle, with a radius of 0.635 mm, into account. Calculations are

performed between r = 0 mm and r = 166 mm, which is 25 times the probe spacing, to minimize the amount of conductive heat reaching the boundary. Commonly 6 mm is used for spacing between the heater probe and the measurement probe (e.g., Ren et al., 2003; Ochsner and Baker, 2008). Therefore, the temperature changes at a node 6 mm away from the center are assumed to represent measurement probe for temperature change. A time step of 0.01s is used. Boundary conditions are set as heat production at the center node and constant temperature at r = 166 mm. The heat production at the center node Q (W m^{-1}) is described as

$$\begin{cases} Q_{r=1} = q' & t \le t_0 \\ Q_{r=1} = 0 & t > t_0 \end{cases} \qquad [8]$$

where q' is heat flux applied at the heater probe (W m^{-1}), and t_0 is heating duration (s). Heat flux q' and heating duration t_0 are set at 12 W m^{-1} and 30 s, respectively. Although larger heat intensity and smaller heating duration has been used for DPHP measurements in unfrozen soil, some studies (Liu and Si, 2011; Tian et al., 2015; Kojima et al., 2016) have suggested that the use of small intensity and long duration is preferred for frozen soil to minimize ice melting. The heat intensity and duration are selected based on Kojima et al. (2016) who report that they provide clear peaks in temperature with time data.

Evaluation of model performance

The performance of the numerical model is evaluated by comparing it to the PILSS (Eq. [9]) at temperatures of 20°C and −20°C;

$$\Delta T = \begin{cases} -\dfrac{q'}{4\pi\lambda}\mathrm{Ei}\left(\dfrac{-r^2C}{4\lambda t}\right) & 0 < t \le t_0 \\ \dfrac{q'}{4\pi\lambda}\left[\mathrm{Ei}\left(\dfrac{-r^2C}{4\lambda(t-t_0)}\right) - \mathrm{Ei}\left(\dfrac{-r^2C}{4\lambda t}\right)\right] & t > t_0 \end{cases} \quad [9]$$

where r is the distance between the heater (center node) and the temperature sensor (mm), ΔT is temperature change at r and t, and Ei is the exponential integral. Model comparisons are made at θ_T of 0.2, 0.3, and 0.4 $m^3\ m^{-3}$. Model performance is evaluated by comparing the maximum temperatures T_m and the times of the maximum temperature t_m for each scenario. The T_m and t_m are strongly associated with C and λ, respectively, and some methods have been proposed to determine C and λ of unfrozen soil from T_m and t_m (Bristow et al., 1994; Knight and Kluitenberg, 2004).

Sensitivity analysis

The numerical solution (Eq. [2]) requires several input values, i.e., initial temperature T_{ini} (°C), λ, C, θ_T, and shape of the FC (θ_s, θ_r, α, and n in Eq. [3]). The input properties T_{ini}, θ_T, and FC are not required to estimate heat transfer in unfrozen soils and, thus, the increase in input values to model heat transfer in partially frozen soil highlights the difficulty of simultaneous determination of λ and C with DPHP methods in partially frozen soils. Soil properties that have high sensitivity to heat pulse induced temperature changes may be determined by DPHP, but those with low sensitivity may be difficult to determine. The sensitivity coefficient values (φ) of each input are described as (Hamby, 1994; Goh and Noborio, 2015);

$$\varphi_j = \frac{\partial y}{\partial x_j}\frac{x_j}{y} \quad [10]$$

where y is the simulated value of ΔT, and x is jth input property. The y is assumed to be T_m, and t_m. The T_{ini}, λ, C, θ_T, θ_s, θ_r, α, and n values are selected for x_j. Simulations are performed at T_{ini} of −0.5°C, −1°C, −2°C, and −4°C, and θ_T of 0.20 m^3 m^{-3}, 0.30 m^3 m^{-3}, and 0.40 m^3 m^{-3}. These temperatures are chosen because DPHP measurement errors have been reported mainly in the temperature range of 0°C to −5°C (Tian et al., 2015; He et al., 2015; Kojima et al., 2016). The water contents are based on field measurements reported by Kojima et al. (2014) where the 0- to 10-cm soil layer water contents in the Nicollet sandy clay loam field range from 0.20 m^3 m^{-3} to 0.40 m^3 m^{-3}.

After the initial simulations, additional simulations using soil properties with ±10% and ±20% errors imposed on input parameters are performed to determine the sensitivity of ΔT to each input parameter. Error of only −5%, instead of −10% and −20%, is imposed on n, since n must be larger than 1, and n values close to 1 produce unrealistic FC curves. The FC curves with error imposed on four parameters are shown in Fig. 2. Significant influences on FC curves occur when errors are imposed on θ_s and n, while the errors imposed on θ_r and α do not affect FC curve shape. Finally, simulations with ±1% and ±2% errors in each input parameter are performed to calculate φ values. The partial derivative in Eq. [10] is determined from the slope of ΔT against input parameters with ±1% and ±2% errors.

Results and Discussion

Evaluation of model performance

Comparisons between the temperature change calculated with PILSS and the numerical model at 20°C and −20°C are shown in Fig. 4. The temperature changes simulated with the numerical solution and PILSS at 20°C were consistent with only slight differences around the time of the maximum temperature. Differences in T_m and t_m of the numerical solution and PILSS at 20°C were at most 0.005°C and 0.8 s, representing 1% and 2% of the T_m and t_m, respectively. The small differences were associated with the fact that the heat capacity of the stainless steel probe was included in the numerical solution but not in PILSS. Temperature changes at later times showed only small differences, which was consistent with the findings reported by Lu et al. (2013), i.e., taking the heating probe properties into account was not critical for late time temperature changes. The numerical solution properly estimated the radial heat transfer. While the numerical solution and PILSS showed consistent temperature changes at 20°C, the temperature changes calculated with the numerical solution at −20°C had smaller T_m and slightly larger t_m than PILSS. The differences in T_m and t_m between the numerical solution and PILSS at −20°C were at most 0.071°C and 1.3 s, representing 11% and 4% of the T_m and t_m, respectively. These differences were associated with the ice melting effect. With the numerical model, the energy was partitioned into latent heat to melt the ice and sensible heat to raise soil temperature in the frozen soil, which resulted in a smaller temperature rise and a delay in heat transfer compared to PILSS. In the case

of −20°C and θ_T of 0.40 $m^3 m^{-3}$, approximately 10% of the applied heat was partitioned into latent heat. The results showed that the numerical solution successfully expressed the effect of ice melting during the DPHP measurement.

Sensitivity analysis

Simulated probe temperature changes at a node 6 mm away from the center (heater probe) for ±10% and ±20% errors imposed onto one of the soil properties at θ_T of 0.30 $m^3 m^{-3}$ and T_{ini} of −1°C are shown in Fig. 5. The temperature changes (0.1°C increase) at T_{ini} of −1°C and θ_T of 0.30 $m^3 m^{-3}$ were smaller than those (0.5°C increase) at T_{ini} of −20°C, because more dynamic ice melting and a larger amount of latent heat occurred at −1°C than at −20°C. Approximately 80% of the applied heat was partitioned into latent heat at −1°C.

Imposing errors onto T_{ini} provided clear differences in ΔT (Fig. 5(a)). With −20%, −10%, 10%, and 20% errors imposed on T_{ini}, errors in ΔT were −0.8°C, −0.9°C, −1.1°C, and −1.2°C, respectively. Errors imposed on T_{ini} influenced both T_m and t_m, e.g., 10% error imposed on T_{ini} caused a 10% (0.01°C) increase in T_m and a 9% (10.6 s) decrease in t_m. This was a result of different partitioning of applied heat at each T_{ini}, i.e., a significant fraction of heat was partitioned into latent heat at negative temperatures close to 0°C, but heat partitioning to latent heat decreased as temperature decreased.

Figures 5(b) and 5(c) show measurement probe temperature changes with errors imposed on

values of λ and C at T_{ini} of −1°C and θ_T of 0.30 m^3 m^{-3}, respectively. Errors imposed on λ created clear differences in t_m but only small differences in T_m, e.g., a 10% increase in λ caused a 8% (10 s) decrease in t_m and a 0.03% (3.3×10^{-5}°C) decrease in T_m. The errors imposed on C resulted in similar temperature changes at the measurement probe. The difference in t_m was difficult to detect visually while small changes in T_m were observed. For example, a 10% error in C caused a 0.6% (0.7 s) change in t_m and a 1% (0.001°C) change in T_m.

The measurement probe temperatures with errors imposed on θ_T at T_{ini} of −1°C and θ_T of 0.30 m^3 m^{-3} are presented in Fig. 5(d). Temperature changes with errors imposed on θ_T showed similar trends to those with errors imposed on λ. Because both λ and C are functions of θ_T, a change in the value of θ_T resulted in changes for both λ and C. Therefore, temperature changes with errors imposed on θ_T included the combined effects of changes in λ and C, i.e., clear increase in t_m and slight decrease in T_m associated with the increase in θ_T, A 10% increase in θ_T caused a 6% (7.6 s) decrease in t_m and a 0.5% (0.0005°C) decrease in T_m. The change in t_m associated with the error imposed on θ_T was smaller than that with the error imposed on λ, and the change in T_m. This was likely because a 10% error in θ_T caused <10% change in λ.

Figure 5(e)-(h) show simulated temperature changes with errors imposed on FC parameters. The impacts of θ_s and n were most significant among the four FC parameters. α caused a minor variation of temperature change, and θ_r had little influence on the temperature change. For example, a 10% error

in θ_s caused a 6% (7.4s) increase in t_m and a 7% (0.007°C) decrease in T_m, while a 10% error in θ_r caused a 0.04% (0.05s) increase in t_m and a 0.1% (0.0001°C) increase in T_m. A 10% error in α caused a 1% (1.4s) decrease in t_m and a 1% (0.001°C) increase in T_m, while a 10% error in n caused a 22% (25.6s) decrease in t_m and a 34% (0.034°C) increase in T_m. In this case, the impacts of the four parameters were associated with the slope of the FC curve at a temperature of −1°C. If an error in the parameter increased the slope of the FC curve, more ice melt occurred and temperature rise was small. From Fig. 2, it can be seen that θ_s and n variations result in dynamic changes in the slope of the FC curve. The slope of the FC curve in each simulation is shown in Table 2. The FC slopes were most affected by the errors in n, followed by those in θ_s. The influence of errors in θ_r on the FC slope was not significant because the given value of θ_r from the fitting of Eq. [3] was 0.01 $m^3\ m^{-3}$, and ±10% and ±20% errors ($\leq$ 0.02 $m^3\ m^{-3}$) were quite small.

Figure 6 shows φ values of t_m and T_m at T_{ini} of −1°C and θ_T of 0.30 $m^3\ m^{-3}$. Only the results at T_{ini} of −1°C and θ_T 0.30 $m^3\ m^{-3}$ were presented because similar trends were observed at other T_{ini} and θ_T values. The absolute values of φ ($|\varphi|$) represented the magnitudes of influence of each parameter on t_m and T_m. The $|\varphi|$ of t_m to n was the largest (2.7), followed by $|\varphi|$ to T_{ini}, λ, θ_T, and θ_s (0.99, 0.93, 0.68, and 0.59, respectively). The $|\varphi|$ values of t_m to α, C, θ_r were small (<0.14) (Fig. 6(a)). Given that the parameters n and θ_s were the main factors changing the slope of FC, the $|\varphi|$ values of those two were relatively large. The T_{ini} also changed the slope of the FC curve dynamically, i.e., a variation in

temperature changed the calculation of ice melting by using different portions of the FC curve, which resulted in large |φ| values from T_{ini}. It was favorable that t_m sensitivity to λ was of similar magnitude to the other high-sensitivity parameters. This suggested the possibility that λ could be accurately determined with DPHP measurements.

The |φ| value of T_m was the largest for n (2.4), followed by T_{ini} (0.99) and θ_s (0.73) (Fig. 6(b)). As before, these were parameters associated with the slope of the FC curve, i.e., parameters that determine the amount of melting ice. The T_m |φ| values of C and of α were small (0.15), and the |φ| values of λ and θ_r were even smaller than those of C and α. This indicated that T_m was dominated by how much ice melted rather than by the C value, and C was thus difficult to determine with T_m of a DPHP measurement.

At T_{ini} of −1°C and θ_T of 0.30 m^3 m^{-3}, the φ value of t_m for λ determined by PILSS was −0.26, and the φ value of T_m for C determined by PILSS was −0.78. Note that PILSS did not account for ice melting. Thus, the |φ| value for λ with the numerical solution (i.e., in frozen soil) was larger than that for λ with PILSS (i.e., in unfrozen soil), while the |φ| value for C with the numerical solution was smaller than that for C with PILSS. These results supported the premise that the determination of λ was more feasible than was the determination of C in frozen soil with DPHP sensors. However, T_m of DPHP in frozen soil was relatively small and the peak of the temperature change was relatively flat, so it could be difficult to detect t_m accurately.

Contours for φ values of t_m to λ and φ values of T_m to C as functions of T_{ini} and θ_T were developed with the contour mapping software SURFER ver. 12 (Golden Software, Inc., Golden, USA) (Fig.7). As temperature decreased, the |φ| values of t_m to λ decreased and became closer to the φ value for λ determined by PILSS, i.e., the amount of ice melting decreased. Alternately, the |φ| values of T_m to C increased as temperature decreased. At relatively high temperatures (i.e., close to 0°C), the |φ| values of T_m to C in frozen soils were smaller than those in unfrozen soils (i.e., PILSS sensitivity), but they began to approach the sensitivity of unfrozen soil as temperature decreased. The |φ| values for θ_s, T_{ini}, and α, i.e., parameters influencing the amount of ice melting, decreased as temperature decreased, and ice melting was reduced, although there were no clear relationships between |φ| for n and T_{ini} or θ_T. The |φ| values for n were large and distributed between 1.5 and 3.6, regardless of T_{ini} and θ_T for the simulated temperature range of −4°C to −0.5°C. However, additional calculations of φ values of t_m for n showed values between 0.55 and 1.1, and φ values of T_m for n showed values between 0.71 and 1.2 at −20°C (data not shown). Given that, the influence of the FC parameters on t_m and T_m were critical in the temperature range between −4°C and −0.5°C, and the influence became weak as temperature decreased.

Our sensitivity analysis revealed that some model input parameters had relatively large influences on the measurement probe temperature changes, while other parameters had relatively small effects. The measurement probe temperature changes were most sensitive to T_{ini}, λ, θ_T, θ_s, and n, and least sensitive to C, θ_r, and α. Both t_m and T_m were sensitive to T_{ini}, θ_s, and n, but only t_m was sensitive to

λ and θ_T,. The results indicated that T_{ini} must be measured carefully. Using high resolution thermocouples or thermistors and datalogging equipment enabled accurate measurement of T_{ini}, so that its value could be determined by measurement. The θ_T showed that φ values of t_m were similar to those for λ, which was because changes in θ_T caused changes in λ as discussed earlier. Therefore, changes in θ_T were not important, and they could be treated as changes in λ. Given that, the sensitive model parameters were λ, θ_s and n. The sensitivity analysis indicated that the DPHP probe temperature changes were determined primarily by λ and FC shape, i.e., θ_s and n were both parameters determining FC shape. This finding pointed to the possibility that λ and FC shape, rather than λ and C, could be determined by inverse analysis with the partially frozen soil numerical model at temperatures close to 0°C.

Because T_m values of the measurement probe were more sensitive to the FC parameters (θ_s and n) than to C, it might be impossible to determine C in partially frozen soil with the DPHP method at temperatures near 0°C. A small variation in FC could mask the influence of C on T_m. Zhang et al. (2011) examined an inverse determination of C in frozen sand with a simple approximation of the FC (two linear functions were applied to describe the FC curve). However, the estimated C values were inaccurate at temperatures between −2 and 0°C. The inaccurate values might be the result of an inaccurate modeling of the FC curve because an actual soil FC curve did not always follow simple approximations. Therefore, accurate modeling of the FC curve was necessary to determine C with DPHP. Nuclear magnetic resonance (NMR) could be used to measure FC curves (Watanabe and Wake, 2009).

However, it was uncertain if NMR measured FC curves could fully represent in-situ FC curves. Improved models for FC curves are needed. In addition, because the FC shows hysteresis (Spaans and Baker, 1996), the modeling of an in-situ FC curve is quite challenging. If accurate FC curve measurements and modeling become available, the determination of C with DPHP may be possible. Otherwise, C should be determined or estimated independently with an alternative method or model.

Conclusions

The aim of this study was to determine the sensitivity of DPHP measurement probe temperature changes in partially frozen soils to corresponding soil conditions and properties, such as T_{ini}, λ, C, θ_T, and FC parameters, θ_s, θ_r, α and n. A numerical solution for radial heat conduction with water phase change was developed, and parameter sensitivity analysis with the model was performed. The sensitivity analysis revealed that for T_{ini} between −4°C and −0.5°C, the temperature change at the measurement probe was sensitive to T_{ini}, λ, θ_T, and FC parameters θ_s and n, but not to C and other FC parameters (i.e., θ_r and α). Because T_m was more sensitive to θ_s and n than to C, it might be impossible to accurately determine C of partially frozen soil with DPHP sensors at temperatures near 0°C. For partially frozen soils at temperatures between −4°C and −0.5°C, λ and FC parameters could be determined by inverse analysis with the numerical model. This sensitivity analysis provided guidance for future studies to further test DPHP sensors in partially frozen soils.

Acknowledgements

This work was supported by the National Science Foundation under Grant 1623806, the Army Research Office Award W911NF1610287, the USDA-NIFA multi-State Project 3188, by Hatch Act, State of Iowa, and State of North Carolina funds.

References

Bilskie, J.R., Horton, R., Bristow, K.L., 1998. Test of a dual-probe heat-pulse method for determining thermal properties of porous materials. Soil Sci. 163, 346-355.

Bristow, K.L., Kluitenberg, G.J., Horton, R., 1994. Measurement of thermal properties with a dual-probe heat-pulse technique. Soil Sci. Soc. Am. J. 58, 1288-1294.

Brooks, R.H., Corey, A.T., 1964. Hydraulic properties of porous media, Hydrology Paper No. 3. Colorado State University, Fort Collings.

Campbell, G.S., Calissendorff, C., Williams, J.H., 1991. Probe for measuring soil specific heat using a heat-pulse method. Soil Sci. Soc. Am. J. 55, 291-293.

de Vries, D.A., 1963. Thermal properties of soils, in: van Wijk, W.R. (Ed), Physics of plant environment. North Holland Publ., Amsterdam, P. 210-235.

Farouki, O.T., 1986. Thermal properties of soils. Trans Tech Publ., Clausthal-Zellerfeld.

Flerchinger, G.N., Saxton, K.E., 1989. Simultaneous heat and water model of a freezing snow-residue-soil system: I. Theory and development. Trans. ASAE 32, 565–571.

Goh, E.G., Noborio, K., 2015. Sensitivity analysis and validation for numerical simulation of water infiltration into unsaturated soil. Int. Sch. Res. Not. 2015, 824721. doi:10.1155/2015/824721

Hamby, D.M., 1994. A review of techniques for parameter sensitivity analysis of environmental models. Environ. Monit. Assess. 32, 135-154.

Hansson, K., Šimůnek, J., Mizoguchi, M., Lundin, L.-C., van Genuchten, M. Th., 2004. Water flow and heat transport in frozen soil: numerical solution and freeze-thaw applications. Vadose Zone J. 3, 693-704.

He, H. Dyck, M., Wang, J., Lv, J., 2015. Evaluation of TDR for quantifying heat-pulse-method-induced ice melting in frozen soils. Soil Sci. Soc. Am. J. 79, 1275-1288.

Heitman, J.L., Horton, R., Sauer, T.J., DeSutter, T.M., 2008a. Sensible heat observations reveal soil water evaporation dynamics. J. Hydrometeorol. 9, 165-171.

Heitman, J.L., Xiao, X., Horton, R., Sauer, T.J., 2008b. Sensible heat measurements indicating depth and

magnitude of subsurface soil water evaporation. Water Resour. Res. 44, W00D05.

Jansson, P.-E., Karlberg, L., 2001. Coupled heat and mass transfer model for soil-plant-atmosphere systems. Royal Institute of Technology, Dept. of Civil and Environmental Engineering, Stockholm.

Kluitenberg, G.J., Ham, J.M., Bristow, K.L., 1993. Error analysis of the heat pulse method for measuring soil volumetric heat capacity. Soil Sci. Soc. Am. J. 57, 1444-1451.

Knight, J.H., Kluitenberg, G.J., 2004. Simplified computational approach for the dual-probe heat-pulse method. Soil Sci. Soc. Am. J. 68, 447-449.

Knight, J.H., Kluitenberg, G.J., Kamai, T., Hopmans, J.W., 2012. Semianalytical solution for dual-probe heat-pulse applications that accounts for probe radius and heat capacity. Vadose Zone J. 11(2), doi:10.2136/vzj2011.0112

Kojima, Y., Heitman, J.L., Flerchinger, G.N., Ren, T., Ewing, R.P. Horton, R., 2014. Field test and sensitivity analysis of a sensible heat balance method to determine soil ice contents. Vadose Zone J. 13(9), Doi:10.2136/vzj2014.04.0036

Kojima, Y., Heitman, J.L., Flerchinger, G.N., Ren, T., Horton, R., 2016. Sensible heat balance estimates of transient soil ice contents. Vadose Zone J. 15(5), doi:10.2136/vzj2015.10.0134

Kurylyk, B.L., Watanabe, K., 2013. The mathematical representation of freezing and thawing processes in variably-saturated, non-deformable soils. Adv. Water Resour. 60, 160-177.

Liu, G., Si, B.C., 2011. Soil ice content measurement using a heat pulse probe method. Can. J. Soil Sci. 91, 235-246.

Lu, Y., Wang, Y., Ren, T., 2013. Using late time data improves the heat-pulse method for estimating soil thermal properties with the pulsed infinite line source theory. Vadose Zone J. 12(4), DOI: 10.2136/vzj2013.01.0011

Ochsner, T.E.,Baker, J.M., 2008. In situ monitoring of soil thermal properties and heat flux during freezing and thawing. Soil Sci. Soc. Am. J. 72, 1025-1032.

Ochsner, T.E., Horton, R., Ren, T., 2001. A new perspective on soil thermal properties. Soil Sci. Soc. Am. J. 65, 1641-1647.

Patanker, S.V., 1980. Numerical heat transfer and fluid flow. Hemisphere, New York.

Putkonen, J. 2003. Determination of frozen soil thermal properties by heated needle probe. Permafrost Periglac. Process. 14, 343-347.

Ren, T., Ochsner, T.E., Horton, R., 2003. Development of thermo-time domain reflectometry for vadose zone measurements. Vadose Zone J. 2, 544-551.

Spaans, E.J.A., Baker, J.B., 1996. The soil freezing characteristic: Its measurement and similarity to the soil moisture characteristic. Soil Sci. Soc. Am. J. 60, 13-19.

Tian, Z., Heitman, J., Horton, R., Ren, T., 2015. Determining soil ice contents during freezing and thawing with thermo-time domain reflectometry. Vadose Zone J. 14(8), doi:10.2136/vzj2014.12.0179

van Genuchten, M.Th. 1980. A closed-form equation for predicting the hydraulic conductivity of unsaturated soils. Soil Sci. Soc. Am. J. 44, 892-898.

Watanabe, K., Wake, T., 2009. Measurement of unfrozen water content and relative permittivity of frozen unsaturated soil using NMR and TDR. Cold Reg. Sci. Technol. 59, 34-41.

Xiao, X., Horton, R., Sauer, T.J., Heitman, J.L., Ren, T., 2011. Cumulative soil water evaporation as a function of depth and time. Vadose Zone J. 10, 1016-1022.

Zhang, Y., Treberg, M., Carey, S.K., 2011. Evaluation of the heat pulse probe method for determining frozen soil moisture content. Water Resour. Res. 47, W05544.

Table 1. Soil information and empirical parameters for Nicollet sandy clay loam. Freezing characteristic curve parameters correspond to Eq. [3].

Textural fractions						Freezing characteristic parameters			
sand	silt	Clay	Organic matter	Bulk density	Specific heat of soil solid	θ_s	θ_r	α	n
----------kg kg^{-1}----------				Mg m^{-3}	J kg^{-1} °C^{-1}	-----m^3 m^{-3}-----			
0.503	0.292	0.205	0.054	1.2	8.79×10^2	0.562	0.01	1671	1.21

Thermal parameters						
c1	c2	c3	c4	c5	F1	F2
0.79	1	14.3	−3	1	3.56	0.68

Table 2. Slope of the freezing characteristic curve at −1°C with error-imposed parameters in Eq. [3].

% error	Error-imposed parameters			
	θ_s	θ_r	α	n
−20	0.020	0.025	0.026	-
−10 (−5 for n)	0.022	0.025	0.025	0.027
0	0.025	0.025	0.025	0.025
10	0.027	0.025	0.024	0.016
20	0.030	0.025	0.024	0.009

Figure Captions

Fig. 1. Discretized areas and nodes are shown. Symbols denote distance from center (r), thermal conductivity of the boundaries (λ), temperature at each node (T), distance between boundaries (Δr), and distance between nodes δr. The subscript i represents the order of nodes.

Fig. 2. Displayed are the observed water retention curve and fitted van Genuchten freezing characteristic model (Eq. [3]) for Nicollet sandy clay loam. The freezing characteristic curves estimated with Eq. [3] with ±10% and ±20% error (only −5%, 10%, and 20% errors for n) are imposed onto the four fitting parameters (a) θ_s, (b) θ_r, (c) α, and (d) n. Two x axes, matric potential and temperature, corresponding to each other via the Clausius-Clapeyron equation (Eq. [4]), are shown.

Fig. 3. Observed thermal conductivity is presented as a function of volumetric water content (θ) and temperature, and the fitted Hansson et al. (2003) model is indicated.

Fig. 4. Temperature changes are calculated with the developed numerical solution and the pulsed infinite line source solution (PILSS) at (a) 20°C and (b) −20°C.

Fig. 5 Simulated temperature changes are presented with errors imposed on soil properties at an initial temperature, T_{ini}, −1°C and total water content, θ_T, 0.30 m^3 m^{-3}. Errors of ±10% and ±20% are imposed onto T_{ini} (a), θ_T (b), thermal conductivity, λ (c), volumetric heat capacity, C (d), freezing characteristic parameters θ_s (e), θ_r (f), and α (g). Errors of −5%, 10%, and 20% are imposed onto freezing

characteristic parameter n (h). Note that the y axis range in panel (h) differs from the others.

Fig. 6. Sensitivity coefficients are indicated of the soil parameters to the elapsed time of maximum temperature t_m and the maximum temperature rise T_m at an initial temperature of −1°C and total water content of 0.30 m^3 m^{-3}. The properties are ordered from left (smallest) to right (largest) in terms of their sensitivities.

Fig. 7 Contours are presented of the sensitivity coefficient of time to maximum temperature t_m to thermal conductivity λ (a), and of maximum temperature T_m to volumetric heat capacity C (b) as functions of initial temperature T_{ini} and total water content θ_T.

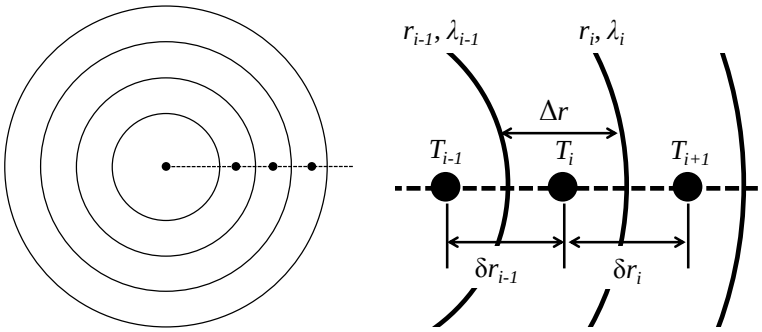

Fig. 1. Discretized areas and nodes are shown. Symbols denote distance from center (r), thermal conductivity of the boundaries (λ), temperature at each node (T), distance between boundaries (Δr), and distance between nodes δr. The subscript i represents the order of nodes.

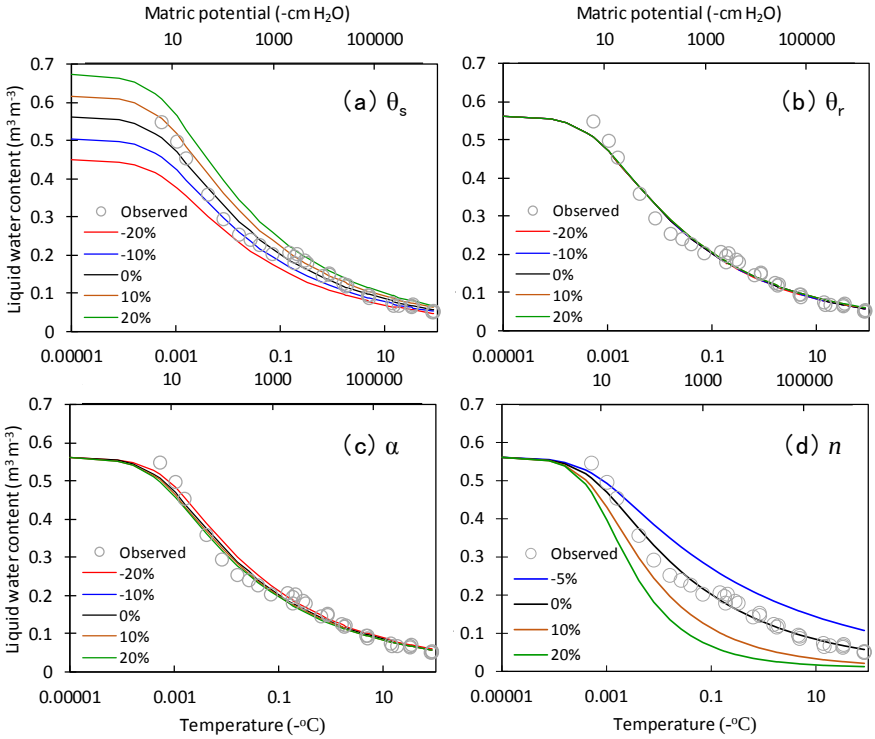

Fig. 2. Displayed are the observed water retention curve and fitted van Genuchten freezing characteristic model (Eq. [3]) for Nicollet sandy clay loam. The freezing characteristic curves estimated with Eq. [3] with ±10% and ±20% error (only −5%, 10%, and 20% errors for *n*) are imposed onto the four fitting parameters (a) θ_s, (b) θ_r, (c) α, and (d) *n*. Two *x* axes, matric potential and temperature, corresponding to each other via the Clausius-Clapeyron equation (Eq. [4]), are shown.

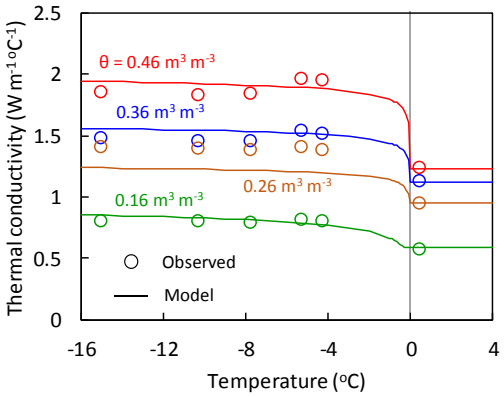

Fig. 3. Observed thermal conductivity is presented as a function of volumetric water content (θ) and temperature, and the fitted Hansson et al. (2003) model is indicated.

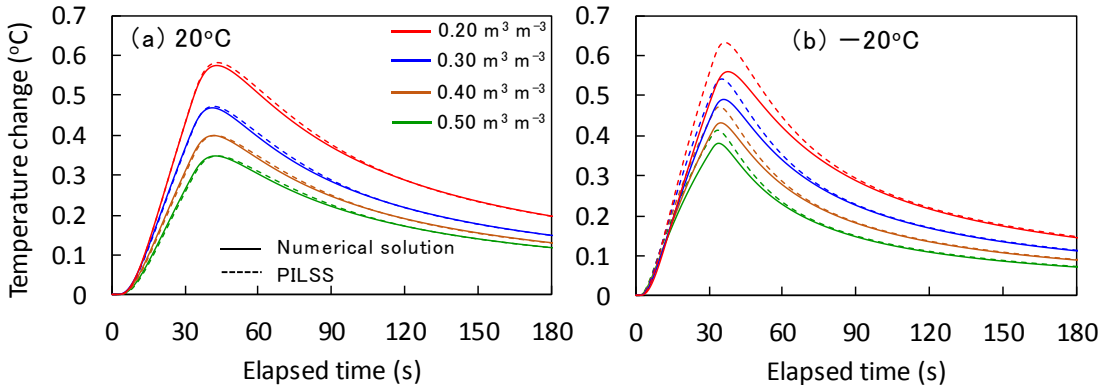

Fig. 4. Temperature changes are calculated with the developed numerical solution and the pulsed infinite line source solution (PILSS) at (a) 20°C and (b) −20°C.

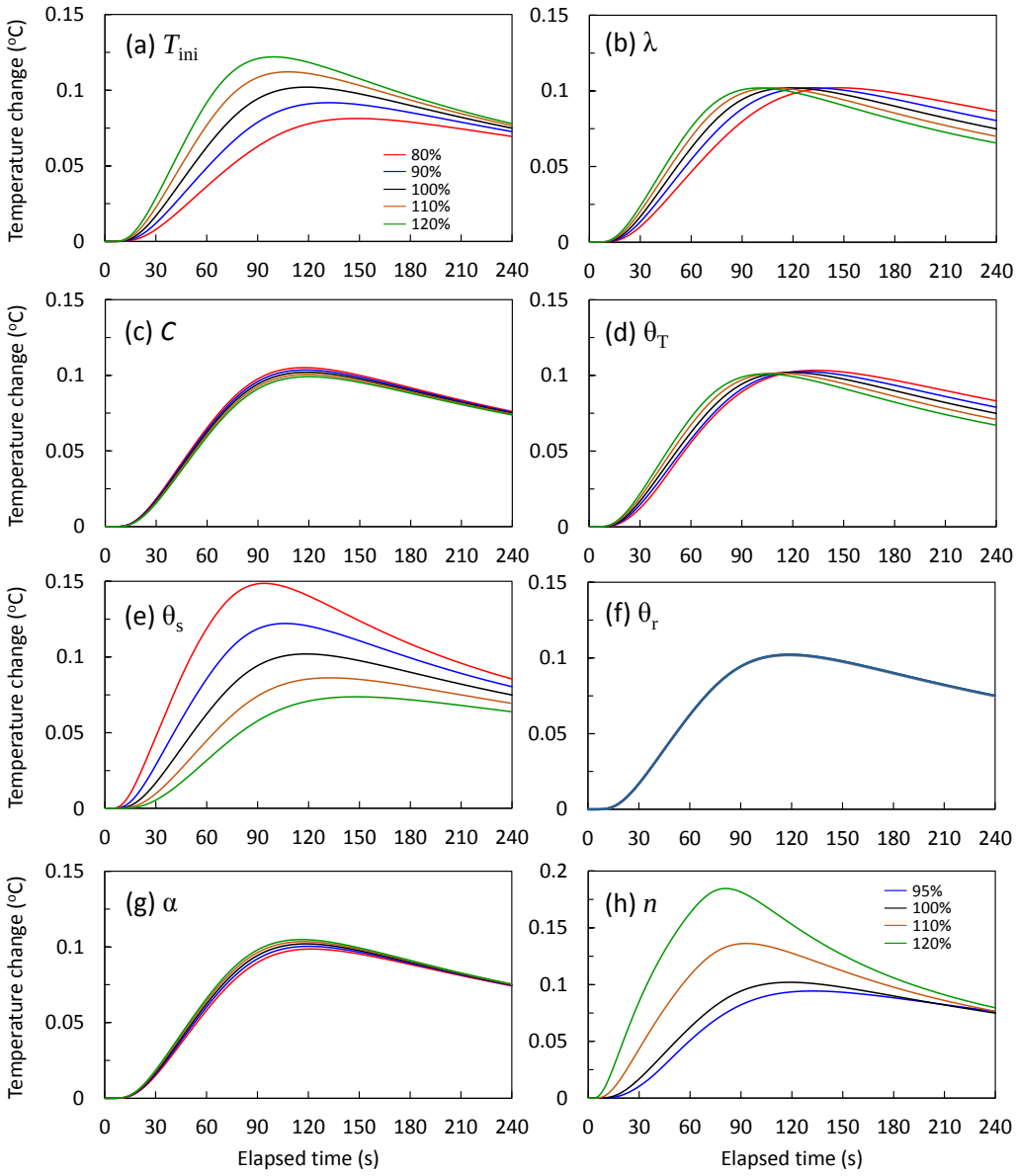

Fig. 5 Simulated temperature changes are presented with errors imposed on soil properties at an initial temperature, T_{ini}, −1°C and total water content, θ_T, 0.30 m^3 m^{-3}. Errors of ±10% and ±20% are imposed onto T_{ini} (a), θ_T (b), thermal conductivity, λ (c), volumetric heat capacity, C (d), freezing characteristic parameters θ_s (e), θ_r (f), and α (g). Errors of −5%, 10%, and 20% are imposed onto freezing characteristic parameter n (h). Note that the y axis range in panel (h) differs from the others.

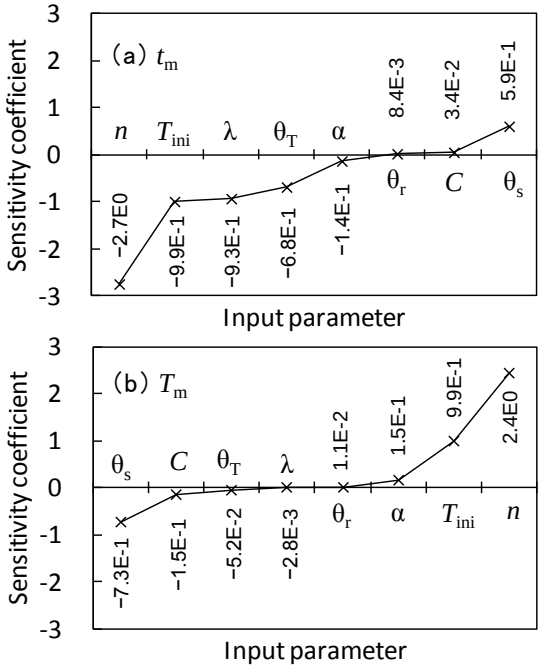

Fig. 6. Sensitivity coefficients are indicated of the soil parameters to the elapsed time of maximum temperature t_m and the maximum temperature rise T_m at an initial temperature of −1°C and total water content of 0.30 m^3 m^{-3}. The properties are ordered from left (smallest) to right (largest) in terms of their sensitivities.

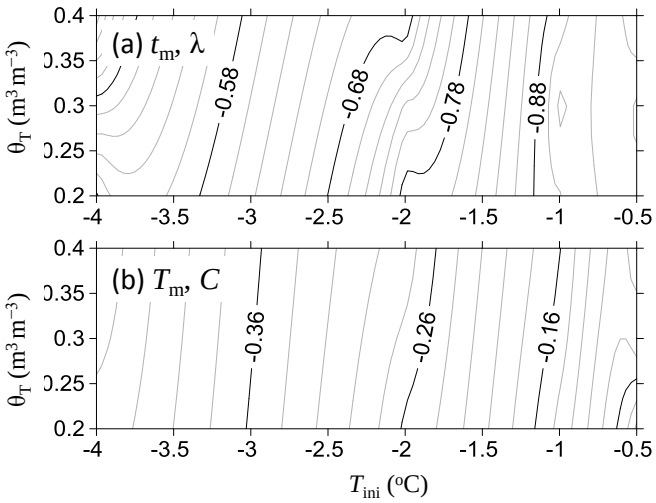

Fig. 7 Contours are presented of the sensitivity coefficient of time to maximum temperature t_m to thermal conductivity λ (a), and of maximum temperature T_m to volumetric heat capacity C (b) as functions of initial temperature T_{ini} and total water content θ_T.

Highlights

- The sensitivity of dual probe heat pulse sensor temperature changes to frozen soil conditions and thermal propertieswas determined.

- The influence of volumetric heat capacityon temperature response to a heat pulse is masked by that of the freezing characteristic.

- Thermal conductivityand freezing characteristicparameters are the best candidate parameters to be determined by the dual probe heat pulse sensor.

- This new result will guide further testing of dual probe heat pulsesensors in partially frozen soils.